Nanoparticles

DOI: 10.1002/anie.200703632

Electrochemical Regeneration of NADH Enhanced by Platinum Nanoparticles**

*Hyun-Kon Song, Sahng Ha Lee, Keehoon Won, Je Hyeong Park, Joa Kyum Kim, Hyuk Lee, Sang-Jin Moon, Do Kyung Kim, and Chan Beum Park**

Herein, we report the application of nanoparticulate platinum (nPt) to enhancing the heterogeneous electron transfer between NAD^+ (nicotinamide adenine dinucleotide, oxidized form) and electrodes in the presence of an organometallic mediator. (Pentamethylcyclopentadienyl-2,2′-bipyridine-chloro)rhodium(III) ($\mathbf{M} = [Cp^*Rh(bpy)Cl]^+$; $Cp^* = C_5Me_5$, bpy = 2,2′-bipyridine) was used as a primary mediator to shuttle electrons between NAD^+ and electrodes. nPt functioned as a homogeneous catalyst and also as a secondary mediator to improve the turnover kinetics of **M**.

Pyridine nucleotides (NAD(P)H) or their oxidized counterparts ($NAD(P)^+$) are used as cofactors that are critically required for redox reactions catalyzed by various oxidoreductases.[1,2] In biocatalytic reactions, NADH should be regenerated to allow the enzymes to continue their turnover. Electrochemical regeneration has been chosen as an attractive strategy that is an alternative to enzymatic regeneration.[3] In electrochemical regeneration, however, the first drawback to overcome is the slow electron transfer between NAD^+ and the electrodes, even at a potential where the reduction of NAD^+ into NADH is thermodynamically favorable. The use of a homogeneous mediator to shuttle electrons between electrodes and NAD^+ can be one solution to solve the problem.[4–6]

The rhodium complex **M** was successfully used as an electron shuttle for NAD^+ in electrolyte, which improved the kinetics of NADH regeneration.[7–9] The active reduced form $\mathbf{M}_{red2}$ that enables NADH to be generated is made through a typical electrochemical/chemical (EC) process (Scheme 1).

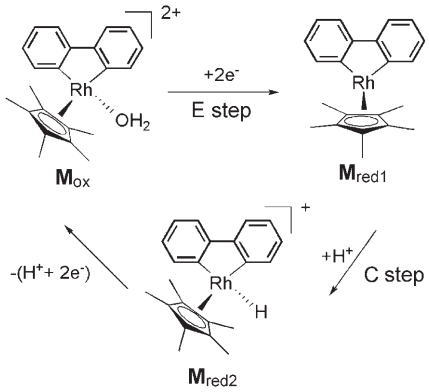

Scheme 1. Molecular structures of three different electrochemical states of **M**.

$\mathbf{M}_{ox}$ is reduced to $\mathbf{M}_{red1}$ by accepting two electrons from the electrodes (E step). Successively, $\mathbf{M}_{red1}$ is chemically converted into $\mathbf{M}_{red2}$ without any change in the total number of electrons, by taking up one proton from solution (C step). NADH is generated from NAD^+ with the active form $\mathbf{M}_{red2}$ by accepting one proton plus two electrons from $\mathbf{M}_{red2}$ and returning $\mathbf{M}_{red2}$ to the initial state $\mathbf{M}_{ox}$ (Scheme 2).

The chemical step from $\mathbf{M}_{red1}$ to $\mathbf{M}_{red2}$ (the uptake of a proton into the ligand sphere of $\mathbf{M}_{red1}$) is the rate-determining step of NADH generation, specifically at high rates, even though it was reported to proceed quite fast.[8] Figure 1a shows cyclic voltammograms obtained at various scan rates. The intensity of the anodic peak increased with scan rate, whereas the peak was not apparently observed at scan rates

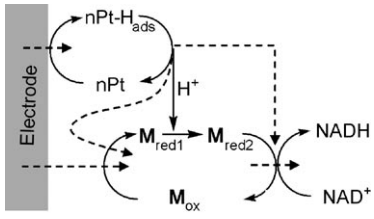

Scheme 2. Indirect electrochemical regeneration of NADH with the primary mediator **M** and its enhancement by proton and electron transfer from nPt to **M**. Dashed arrows indicate electron transfer.

[*] S. H. Lee, J. H. Park, Prof. D. K. Kim, Prof. C. B. Park
Department of Materials Science and Engineering
Korea Advanced Institute of Science and Technology
373-1 Guseong-dong, Yuseong-gu, Daejeon 305-701 (Korea)
Fax: (+82) 42-869-3310
E-mail: parkcb@kaist.ac.kr
Prof. K. Won
Department of Chemical and Biochemical Engineering
Dongguk University
26 Pil-dong 3-ga, Jung-gu, Seoul 100-715 (Korea)
J. K. Kim, Dr. H. Lee, Dr. S.-J. Moon
Korea Research Institute of Chemical Technology (KRICT)
100 Jang-dong, Yuseong-gu, Daejeon 305-343 (Korea)
Dr. H.-K. Song[+]
Division of Engineering
Brown University, Providence, RI 02912 (USA)
[+] Present address: Battery R&D, LG Chem Ltd.
Research Park, 104-1 Moonji-dong, Yuseong-gu, Daejeon 305-380 (Korea)

[**] This work was supported by the Korea Energy Management Corporation (2005-C-CD11-P-04) and the Korea Research Foundation (KRF-2006-331-D00113).

Supporting information for this article is available on the WWW under http://www.angewandte.org or from the author.

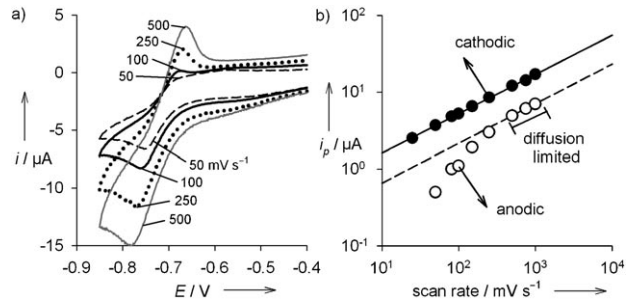

Figure 1. a) Cyclic voltammograms of **M** (500 μM) in phosphate buffer (100 mM) at pH 8.2. Scan rates are indicated in $mV s^{-1}$. b) Scan rate dependency of cathodic and anodic peak currents obtained from (a). Slopes of the lines were estimated at 0.5.

less than $100 mV s^{-1}$. At slow anodic potential sweep, the C step proceeds faster than the E step so that there is no chance for $\mathbf{M}_{red1}$ to donate electrons to the electrode. In fast scans (rate above $500 mV s^{-1}$), however, $\mathbf{M}_{red1}$ is electrochemically oxidized to $\mathbf{M}_{ox}$ before the C step proceeds, as the electron-transfer rate between $\mathbf{M}_{red1}$ and electrodes is controlled by the scan rate and is faster than the rate of the chemical reaction.

The anodic peak current i_p followed the dependency on scan rate of conventional faradaic processes ($i_p \propto [\text{scan rate}]^{0.5}$) only at scan rates higher than $500 mV s^{-1}$, which indicates that $\mathbf{M}_{red1}$ was totally converted to $\mathbf{M}_{ox}$ by the E step (Figure 1b). The peak currents at scan rates less than $500 mV s^{-1}$ deviated from the extrapolated lines fitting peak currents at the three largest scan rates, because $\mathbf{M}_{red1}$ was partly converted to $\mathbf{M}_{red2}$ by the C step. Therefore, the kinetics of proton uptake in the C step should be enhanced to achieve efficient formation of $\mathbf{M}_{red2}$, which is active for NADH generation.

Platinum has been extensively used to reduce protons in electrolytes to hydrogen (hydrogen evolution reaction, HER) and also to oxidize hydrogen to protons in fuel cells.[10,11] The main reason that makes the platinum catalyst superior to other alternative metals is that protons are adsorbed onto platinum atoms. The intermediate state Pt-H_{ads} makes the H^+/H_2 reaction kinetically more favorable, which results in a decrease of overpotential.

Metal–H_{ads} species, including Pt-H_{ads}, were reported to be able to function as a reducing agent for organic molecules, markedly in their nanoparticulate form. Platinum nanoparticles with adsorbed hydrogen atoms (nPt-H_{ads}) were used to reduce the lucigenin cation to its monocation radical in the potential range of the HER.[12] Also, other metal nanoparticle–H_{ads} species were reported to work as a reducing agent:[13,14] nAg-H_{ads} to reduce CH_2Cl_2 to CH_3Cl or Tl^+ to Tl^0; nPd-H_{ads} to reduce Pt^{4+} or Pt^{2+} into Pt^0.

Based on an understanding of the intermediate Pt-H_{ads}, we added nPt to the single-mediator strategy of $\mathbf{M} + NAD^+$. nPt was introduced to play two functional roles in our tandem strategy: 1) the homogeneous catalyst responsible for catalyzing the proton uptake reaction of $\mathbf{M}_{red1}$ to $\mathbf{M}_{red2}$, and 2) the secondary mediator to shuttle electrons from electrodes to $\mathbf{M}_{ox}$. Scheme 2 shows the working mechanism of our tandem-mediator strategy that includes nPt as well as **M**. These two mediators are reduced to nPt-H_{ads} and $\mathbf{M}_{red1}$ at −0.8 V. nPt-H_{ads} returns to nPt by donating a proton to $\mathbf{M}_{red1}$ and an electron to $\mathbf{M}_{ox}$ or NAD^+.

Figure 2a and b shows the change of voltammetric features before and after the addition of nPt to the single-mediator systems (**M** or $\mathbf{M} + NAD^+$). The reduction potential

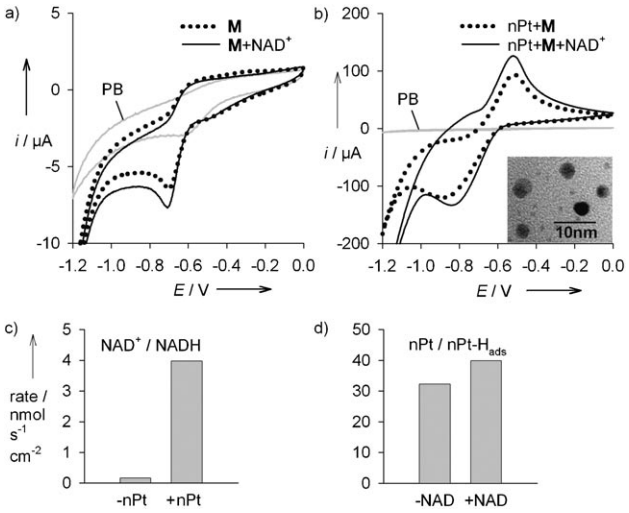

Figure 2. a,b) Cyclic voltammograms of solutions of a) **M** and b) nPt + **M** in the absence and presence of NAD^+. nPt (0.6 mM), **M** (0.5 mM), and NAD^+ (0.5 mM) were used in phosphate buffer (100 mM) at pH 7.0. GC electrodes were used as working electrodes. The potential was scanned at $100 mV s^{-1}$. Inset in (b): transmission electron microscopy image of nPt. c,d) Conversion rates at −0.8 V of c) NAD^+ to NADH in the absence and presence of nPt and d) nPt to nPt-H_{ads} in the absence and presence of NAD^+. The rates ($= \Delta i/nFA$; n = number of electrons, F = Faradaic constant, A = electrode area) were calculated from the difference of the cathodic currents at −0.8 V (in a,b) between $\mathbf{M} + NAD^+$ and **M** for "−nPt" in (c); between nPt + **M** + NAD^+ and nPt + **M** for "+nPt" in (c); between nPt + **M** and **M** for "−NAD^+" in (d); and between nPt + **M** + NAD^+ and $\mathbf{M} + NAD^+$ for "+NAD^+" in (d).

at the cathodic peak current (E_{pc}) of **M** was estimated at −0.7 V in the absence or presence of NAD^+ (Figure 2a). After addition of nPt, the cyclic voltammograms were totally changed. The cathodic and anodic waves shown in Figure 2b arise mostly from adsorption and desorption of protons on nPt with $E_{pc} = -0.85$ to −0.9 V and the oxidation potential at the anodic peak current $E_{pa} = -0.52$ V.[10]

The conversion rates of NAD^+ to NADH (Figure 2c) or nPt to nPt-H_{ads} (Figure 2d) on electrodes were calculated from the difference of cathodic currents at −0.8 V (the working potential used to generate NADH). The addition of nPt enhanced the rate of NADH generation 25 times (rate difference = $3.82 nmol s^{-1} cm^{-2}$). Also, the rate of nPt reduction on electrodes increased 25% in the presence of NAD^+ when compared with that in the absence of NAD^+ (rate difference = $7.64 nmol s^{-1} cm^{-2}$).

The amount of NADH was measured spectroscopically at −0.8 V in the absence or presence of various concentrations of nPt. The amount increased with nPt concentration and

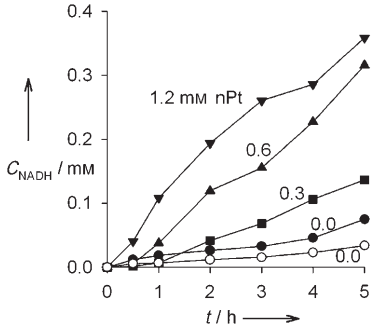

Figure 3. Temporal change of NADH concentration (C_{NADH}) in the absence or presence of nPt. NAD^+ (1 mM) and **M** (500 μM) were used; the concentrations of nPt are indicated. The solutions for all experiments were stirred at 340 rpm (except for ○, when the mixture was not stirred). For electrodes and buffer solutions see Figure 2.

stirring rate (Figure 3). The concentration of NADH measured 5 h after the potential was applied increased five times in the presence of 1.2 mM nPt when compared with that in the absence of nPt. The NADH generated with nPt and **M** proved to work effectively with glutamate dehydrogenase, an oxidoreductase, for the synthesis of L-glutamate from α-ketoglutarate in preliminary experiments.

To confirm the nanoparticulate contribution of nPt to the generation of NADH, various flat and bulky disk electrodes including platinum were tested as the working electrode for NADH generation in the presence of **M**. A very small amount of NADH was generated on these bulky disk electrodes (Figure 4a). For comparison, the amount of NADH generated on glassy carbon (GC) disk electrodes in the presence of 1.2 mM nPt under the same conditions was 0.2 mM (Figure 3).

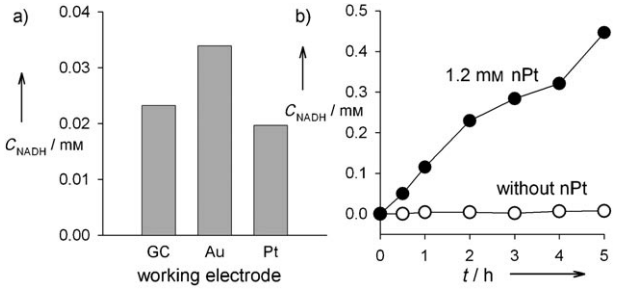

Figure 4. a) Concentration of NADH generated on various working electrodes in a solution of **M** and NAD^+, stirred at 340 rpm, at −0.8 V for 2 h. b) Temporal change of concentration of NADH generated on Pt working electrodes in the absence or presence of nPt. Solutions were stirred at 340 rpm at −0.8 V during NADH generation. **M** (0.5 mM) and NAD^+ (1 mM) were used in phosphate buffer (100 mM) at pH 7.0 for all experiments.

The platinum disk electrode was even less efficient for NADH generation than GC and gold disk electrodes. On the other hand, the addition of nPt to the solution including **M** and NAD^+ resulted in an increase of the amount of NADH generated on the platinum disk electrode (Figure 4b). Therefore, the catalytic (proton donation) and reducing (electron donation) power of nPt can be said to originate from its nanoparticulate feature. The possibility that the increase in the amount of generated NADH is mainly a result of the increase in surface area through adsorption of nPt on the working electrodes should be rejected, because there were no significant differences in the amounts of NADH when using bare and nPt-adsorbed GC electrodes.

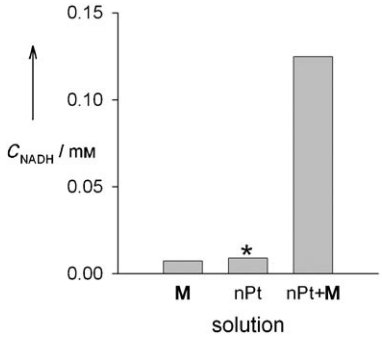

Figure 5. Concentration of NADH generated on a GC working electrode in a solution including **M**, nPt, or nPt + **M**. The solution was stirred at 340 rpm at −0.8 V for 1 h prior to addition of NAD^+ (1 mM). A potential was not applied after adding NAD^+. The asterisk indicates that the same amount of NADH was produced when **M** and NAD^+ were added. nPt (0.6 mM) and **M** (0.5 mM) were used in phosphate buffer (100 mM) at pH 7.0.

To confirm the roles of nPt in the proposed mechanism, prereduced solutions were used to generate NADH without applied potential (Figure 5). If $\mathbf{M_{ox}}$ in solution were totally reduced to $\mathbf{M_{red2}}$, 0.5 mM NADH would be generated after addition of NAD^+ to the prereduced solution. However, the amount of NADH generated in the solution of **M** was estimated as a very dilute concentration of less than 0.01 mM. nPt directly reduced NAD^+ to NADH even if a very small amount of NADH was generated. There were no significant differences of the NADH concentration between solutions including only **M** and only nPt. On the other hand, a synergistic effect was observed in the mixture of nPt and **M**. The amount of NADH generated increased about 20 times (0.125 mM NADH), thus indicating that nPt enhanced the formation of $\mathbf{M_{red2}}$.

In conclusion, nPt was used as a homogeneous catalyst and simultaneously as a secondary mediator for NADH regeneration in the presence of the primary mediator **M**. It enhanced the rate of NADH generation by donating protons and electrons to **M**. We expect that the use of nPt could be extended to the reduction of other chemicals, even in proton-deficient environments (high pH).

Experimental Section

The rhodium complex **M** was synthesized by the method of Kolle and Gratzel.[15] The nPt was prepared by citrate reduction of potassium tetrachloroplatinate.[16,17] An aqueous solution of sodium citrate (30 mL, 680 mM) was added to a boiling aqueous mixture of K_2PtCl_4 (120 mL, 11.5 mM) and polyvinylpyrrolidone (3 g, molecular weight 10k) for 4 h.

To sweep the potential in cyclic voltammograms or to apply constant potential for generating NADH, a single-compartment cell was configured with three electrodes: a GC disk (working, 0.03 cm^2), a platinum wire (counter), and an Ag/AgCl (reference, 0.197 V versus normal hydrogen electrode) connected to a potentiostat/galvanostat (EG&G, Model 273A). All potentials are reported versus Ag/AgCl. The concentration of NADH was estimated from the difference of the absorbance at 340 nm before and after adding NAD^+.

Received: August 9, 2007
Revised: October 10, 2007
Published online: January 25, 2008

Keywords: electron transfer · homogeneous catalysis · NADH · nanoparticles · platinum

[1] E. Siu, K. Won, C. B. Park, *Biotechnol. Prog.* **2007**, *23*, 293.
[2] W. A. van der Donk, H. Zhao, *Curr. Opin. Biotechnol.* **2003**, *14*, 421.
[3] F. Hollmann, A. Schmid, *Biocatal. Biotransform.* **2004**, *22*, 63.
[4] H. Jaegfeldt, A. Torstemsson, L. Gorton, G. Johansson, *Anal. Chem.* **1981**, *53*, 1979.
[5] J. Wang, J. Liu, *Anal. Chim. Acta* **1993**, *284*, 385.
[6] J. Wang, P. V. A. Pamidi, M. Jiang, *Anal. Chim. Acta* **1998**, *360*, 171.
[7] R. Ruppert, S. Herrmann, E. Steckhan, *Tetrahedron Lett.* **1987**, *28*, 6583.
[8] F. Hollmann, A. Schmid, E. Steckhan, *Angew. Chem.* **2001**, *113*, 190; *Angew. Chem. Int. Ed.* **2001**, *40*, 169.
[9] K. Vuorilehto, S. Lütz, C. Wandrey, *Bioelectrochemistry* **2004**, *65*, 1.
[10] N. Nanbu, F. Kitamura, T. Ohsaka, K. Tokda, *J. Electroanal. Chem.* **2000**, *485*, 128.
[11] A. Henglein, B. Lindig, J. Westerhausen, *J. Phys. Chem.* **1981**, *85*, 1627.
[12] J. Z. Guo, H. Cui, S. L. Xu, Y. P. Dong, *J. Phys. Chem. C* **2007**, *111*, 606.
[13] A. Henglein, *J. Phys. Chem.* **1979**, *83*, 2858.
[14] Y. Wang, N. Toshima, *J. Phys. Chem. B* **1997**, *101*, 5301.
[15] F. Hollmann, B. Witholt, A. Schmid, *J. Mol. Catal. B* **2002**, *19–20*, 167.
[16] D. N. Furlong, A. Launikonis, W. H. F. Sasse, *Chem. Soc. Faraday Trans. 1* **1984**, *80*, 571.
[17] I. Okura in *Encyclopedia of Nanoscience and Nanotechnology*, *Vol. 8* (Ed.: H. S. Nalwa), American Scientific Publishers, **2004**, p. 41.

